



HHS Public Access

Author manuscript

Proc IEEE Int Symp Biomed Imaging. Author manuscript; available in PMC 2017 January 16.

Published in final edited form as:

Proc IEEE Int Symp Biomed Imaging. 2015 April ; 2015: 1284–1287. doi:10.1109/ISBI.2015.7164109.

NUCLEI SEGMENTATION VIA SPARSITY CONSTRAINED CONVOLUTIONAL REGRESSION

Yin Zhou^{1,4}, Hang Chang^{1,3,†}, Kenneth E. Barner⁴, and Bahram Parvin^{1,2,3,†}

¹Life Science Division, Lawrence Berkeley National Laboratory, Berkeley, CA, U.S.A

²Biomedical Engineering Department, University of Nevada, Reno, NV, U.S.A

³Department of Electrical and Computer Engineering, University of California, Riverside, U.S.A

⁴University of Delaware, Newark, DE, U.S.A

Abstract

Automated profiling of nuclear architecture, in histology sections, can potentially help predict the clinical outcomes. However, the task is challenging as a result of nuclear pleomorphism and cellular states (e.g., cell fate, cell cycle), which are compounded by the batch effect (e.g., variations in fixation and staining). Present methods, for nuclear segmentation, are based on human-designed features that may not effectively capture intrinsic nuclear architecture. In this paper, we propose a novel approach, called sparsity constrained convolutional regression (SCCR), for nuclei segmentation. Specifically, given raw image patches and the corresponding annotated binary masks, our algorithm jointly learns a bank of convolutional filters and a sparse linear regressor, where the former is used for feature extraction, and the latter aims to produce a likelihood for each pixel being nuclear region or background. During classification, the pixel label is simply determined by a thresholding operation applied on the likelihood map. The method has been evaluated using the benchmark dataset collected from The Cancer Genome Atlas (TCGA). Experimental results demonstrate that our method outperforms traditional nuclei segmentation algorithms and is able to achieve competitive performance compared to the state-of-the-art algorithm built upon human-designed features with biological prior knowledge.

Index Terms

Nuclear/Background classification; convolutional neural network; sparse coding; H&E tissue section

1. INTRODUCTION

Nuclear morphometry reflects cell type, aberration in genome, and potential stress as a result of changes in the micro-environment. For example, in Glioblastoma Multiforme (GBM), nuclear segmentation can help differentiate round oligodendroglioma from elongated and irregular morphology of astrocytoma. In general, (i) cancer nuclei tend to be larger, and if

[†]Corresponding authors: hchang@lbl.gov; b_parvin@lbl.gov.

coupled with high chromatin content, they may indicate aneuploidy; (ii) cellular density can be the result of rapid proliferation; (iii) nuclear texture can be the surrogate for fluctuation of heterochromatin patterns; and (iv) cytoplasmic signature (immediately around the nucleus) can reveal stress related macromolecules that are being secreted. Furthermore, nuclear heterogeneity can potentially play an important role on survival and response to therapy. If nuclear segmentation is successful, it then can be applied to a large scale cohort of hematoxylin and eosin (H&E) stained histology sections, for morphometric subtyping and subsequently the association of each computed subtype to the clinical information. Simultaneously, derived representations (*e.g.*, meta-features), from cell-by-cell analysis, can also be leveraged to probe for heterogeneity and its underlying molecular basis, which can help reveal tumor plasticity (*e.g.*, adaptation to environmental factors), potential peripheral molecular drivers, and drug resistivity.

It is well known that automated segmentation is typically hindered by large amount of technical variations and biological heterogeneities, which are prevalent within large-scale datasets, such as The Cancer Genome Atlas (TCGA). In this paper, we propose a novel approach, called sparsity constrained convolutional regression (SCCR) to potentially test the limit on the performance of segmentation techniques and to overcome the intrinsic complexities of the problem per previous research [1–7]. Given raw image patches and the corresponding annotated binary masks, SCCR jointly learns a convolutional filter bank and a linear mapping with sparsity constraint. The filter bank is a set of specialized feature detectors and is applied to extract pixel-wise feature vectors. The convolutional regression prediction is computed as the inner product between the feature vector and learned weights. By applying the prediction score into a simple decision function, the pixel label can then be determined.

Organization of this paper is as follows: Section 2 reviews previous research. Section 3 describes the details of the proposed framework. Section 4 presents our preliminary experimental results. Lastly, Section 5 concludes the paper and points out future directions.

2. RELATED WORK

The major difficulties towards accurate nuclei segmentation are technical variations (*e.g.*, fixation, staining) and biological heterogeneities (*e.g.*, cell type, cell state). To address this challenging problem, researchers have made a significant amount of effort by introducing techniques from image processing, computer vision and machine learning. Some representative approaches are fuzzy clustering [1], adaptive thresholding followed by morphological filtering [2], hybrid color and texture analysis followed by learning and unsupervised clustering [3], color separation followed by optimum thresholding and learning [4], level set method combining gradient information [5], graph cut method based on seed detection [6]. Color decomposition is a common preprocessing technique to accentuate the nuclear dye. Thresholding and clustering are based on the assumption that all nuclear regions in the image have consistent chromatin content, which in practice, however, does not hold, due to the following reasons: 1) different cell type and cell state may cause significant variations in chromatin content; 2) the overlapping and clumping of cells may cause distortion to the underlying chromatin content. In addition, aforementioned methods are

usually applied to a small dataset collected from a single laboratory and therefore their capability of overcoming technical variations is limited.

Recent years have witnessed increasing popularity of unsupervised feature learning due to its superior performance in many computer vision tasks [8–13]. Therefore, we are motivated to explore its capability for nuclei segmentation.

3. PROPOSED METHOD

3.1. Training Algorithm

We consider the nuclei segmentation as a binary classification problem at pixel level. Let

$\mathbf{X} = \{\mathbf{x}^i\}_{i=1}^N$ be a training set containing N 2D images with dimension $m \times n$. Let

$\mathbf{Y} = \{\mathbf{y}^i\}_{i=1}^N$ be the set of N binary masks, where \mathbf{y}^i is an $m \times n$ binary matrix corresponding to image \mathbf{x}^i , and each pixel $y_{j,k}^i \in \{0, 1\}$ in \mathbf{y}^i indicates the label of the pixel $x_{j,k}^i$ in image \mathbf{x}^i .

Here, we use $y_{j,k}^i = 1$ to denote the nuclear region and use $y_{j,k}^i = 0$ to represent the

background. Let $\mathbf{D} = \{\mathbf{d}_k\}_{k=1}^K$ be the 2D convolutional filter bank consisting of K filters, where each \mathbf{d}_k is an $h \times h$ convolutional kernel. Let $\mathbf{w} = [w_1, \dots, w_K]^T \in \mathbb{R}^K$ be the vector containing K linear combination coefficients, where the k^{th} coefficient w_k is related to the k^{th} filter $\mathbf{d}_k \in \mathbf{D}$. Our goal therefore is simultaneously achieving two objectives: (I) to learn a set of nuclei feature detectors \mathbf{D} that can capture intrinsic cellular morphometric patterns, and (II) to elucidate a sparse representation \mathbf{w} , which maps the feature vector extracted at each pixel to its label. The optimization problem is formulated as

$$\min_{\mathbf{D}, \mathbf{w}} \mathcal{L} = \sum_{i=1}^N \|\mathbf{y}^i - \sum_{k=1}^K w_k \sigma(\mathbf{d}_k * \mathbf{x}^i)\|_{\text{F}}^2 + \alpha \sum_{k=1}^K \|\mathbf{d}_k\|_{\text{F}}^2 + \beta \|\mathbf{w}\|_1 \quad (1)$$

where the first term represents the segmentation error, the second term is a regularization term for penalizing the model complexity in terms of filter bank energy, and the third term is ℓ_1 regularization term included for enforcing the linear representation vector \mathbf{w} to be sparse; α, β are positive regularization constants; σ denotes the sigmoid function; $*$ is the 2D convolution operator. Note that in contrast to traditional convolutional neural network, our optimization object includes the ℓ_1 regularization term which enables feature selection [14] and thus allows the filters to capture salient nuclear patterns.

We solve Eq. (1) by alternatively optimizing the two variables, *i.e.*, iteratively performing the two steps, that is, first compute \mathbf{w} and then update \mathbf{D} . For the purpose of handling large-scale dataset, we follow the mini-batch based training protocol [15], *i.e.*, in each iteration, computing the gradient based on a small subset of the dataset. Specifically, we use the conjugate gradient method [16] to solve for the sparse representation vector \mathbf{w} . On updating the convolutional filter bank \mathbf{D} , we use the Limited memory BFGS (L-BFGS) for efficient estimation of the gradient. The optimization procedure is sketched in Algorithm 1.

Alternative methods for updating the dictionary can be found in [17, 18]. Note that the

objective of Eq. (1) is convex with respect to \mathbf{w} but it is not convex with respect to \mathbf{D} due to the nonlinear sigmoid function; therefore, optimization can only guarantee the convergence to a local minima. However, in practice, achieving local minima is sufficient to generate satisfactory performance. Figure 1 illustrates a subset of learned filters from the TCGA segmentation benchmark dataset.

3.2. Decision Function

Having trained the proposed SCCR model, a test image \mathbf{x} of dimension $p \times q$ can be labeled in three steps. First, compute the convolutional regression prediction as

$$\mathbf{z} = \sum_{k=1}^K w_k \sigma(\mathbf{d}_k * \mathbf{x}) \quad (2)$$

Second, feed the prediction \mathbf{z} into sigmoid function to squash the value of every pixel within the range of (0, 1). Finally, the label of pixel at location (i, j) for all $i = 1, \dots, p$ and $j = 1, \dots, q$ is predicted according to the following decision rule

Algorithm 1

Training Algorithm

Input: Training image set \mathbf{X} , training binary mask set \mathbf{Y} , filter bank size K , mini-batch size T , regularization constants α and β

Output: Convolutional filter bank \mathbf{D} , coefficient vector \mathbf{w}

- 1: **Initialize:** $\mathbf{D} \sim \mathcal{N}(0, 1)$, $\mathbf{w} \leftarrow 0$
 - 2: **repeat**
 - 3: Generate a random index set $\Omega \subset \{1, 2, \dots, N\}$ containing $|\Omega| = T$ indices
 - 4: Fixing \mathbf{D} , compute \mathbf{w} by solving

$$\mathbf{w} \leftarrow \underset{\mathbf{w}}{\operatorname{argmin}} \sum_{i \in \Omega} \|\mathbf{y}^i - \sum_{k=1}^K w_k \sigma(\mathbf{d}_k * \mathbf{x}^i)\|_F^2 + \beta \|\mathbf{w}\|_1$$
 - 5: Fixing \mathbf{w} , update \mathbf{D} over the same training subset as $\mathbf{D} \leftarrow \mathbf{D} - \mu \nabla_{\mathbf{D}} \mathcal{L}(\mathbf{D}, \mathbf{w})$
 - 6: **until** Convergence (maximum iterations reached or objective function threshold)
-

$$\text{Label}(x_{i,j}) = \begin{cases} 1 & \text{if } \sigma(z_{ij}) \geq 0.5 \\ 0 & \text{otherwise} \end{cases} \quad (3)$$

where $x_{i,j}$ and $z_{i,j}$ represent the pixel at location (i, j) in \mathbf{x} and \mathbf{z} respectively.

4. EXPERIMENT

The Cancer Genome Atlas (TCGA) is a publicly accessible repository providing a rich amount of whole mount tumor sections that are collected from different laboratories. Among

the images, there exist significant technical and biological variations. The proposed SCCR is evaluated over 21 1000-by-1000 Glioblastoma Multiforme (GBM) image samples (20X), which are manually selected to capture the diversity in the cohort. Each image is annotated as a binary mask of nuclei versus background. As a pre-processing step, color decomposition [19] was adopted to accentuate the nuclear dye, which generates two frames (*i.e.*, the nuclear and the protein channels) from the original RGB image. For the task of segmentation, only the nuclear channel is used.

From the 21 image samples, we randomly cropped 1400 image patches¹ and the corresponding binary masks as training set. The image patches and the binary masks are of size 64-by-64. For training, we empirically set $K = 1500$, $T = 200$, $\alpha = 10^{-4}$, $\beta = 0.1$. We evaluate the proposed SCCR using all the 21 1000-by-1000 images and compare it with several methods reported in the literature [20–22]. The results are summarized in Table 1. Our method outperforms traditional nuclei segmentation algorithms [20, 22] and is very competitive with one of the state-of-the-art algorithm [21]. Note that unlike the algorithm in [21], which is built upon human engineered prior knowledge. Proposed SCCR is a generic feature learning model and may be applicable to segmentation tasks of other tumor types. Figure 2 illustrates some examples of the original images, corresponding SCCR predictions, and final segmentation results. And the computational cost per image (1000-by-1000 pixels) is less than 40 seconds.

5. CONCLUSION AND FUTURE WORK

In this paper, we propose a novel method (SCCR) for nuclei segmentation. The proposed method addresses the nuclei segmentation as a pixel classification problem, by jointly learning a convolutional filter bank and a linear mapping with sparsity constraint. Compared to previous frameworks with human-engineered features, our method does not rely on prior knowledge and therefore could be potentially applicable to segmentation tasks of different tumor types. Experimental results demonstrate that SCCR outperforms several traditional nuclei segmentation algorithms and achieves very competitive performance compared to one of the state-of-the-art approaches based on biological prior knowledge.

Future work includes i) increasing the training scale for possible improvement of performance; ii) applying SCCR on other benchmark datasets (both 2D and 3D) for extensive evaluation; and iii) further evaluating the proposed method and comparing with deep learning models (e.g., convolutional neural network [8])

Acknowledgments

This work was supported by NIH grant R01 CA140663 carried out at Lawrence Berkeley National Laboratory under Contract No. DE-AC02-05CH11231 with the University of California.

¹Image patches were cropped at nuclear centers, and ~ 10% nuclei were randomly selected for training.

References

1. Latson L, Sebek N, Powell K. Automated cell nuclear segmentation in color images of hematoxylin and eosin-stained breast biopsy. *Analytical and Quantitative Cytology and Histology*. 2003; 26(6): 321–331.
2. Ballaro B, Florena A, Franco V, Tegolo D, Tripodo C, Valenti C. An automated image analysis methodology for classifying megakaryocytes in chronic myeloproliferative disorders. *Medical Image Analysis*. 2008; 12:703–712. [PubMed: 18550417]
3. Datar M, Padfield D, Cline H. Color and texture based segmentation of molecular pathology images using HSOMs. *ISBI*. 2008:292–295.
4. Chang H, Defilippis RA, Tlsty TD, Parvin B. Graphical methods for quantifying macromolecules through bright field imaging. *Bioinformatics*. 2009; 25(8):1070–1075. [PubMed: 18703588]
5. Fatakdawala H, Xu J, Basavanahally A, Bhanot G, Ganesan S, Feldman F, Tomaszewski J, Madabhushi A. Expectation-maximization-driven geodesic active contours with overlap resolution (EMaGACOR): Application to lymphocyte segmentation on breast cancer histopathology. *IEEE Transactions on Biomedical Engineering*. 2010; 57(7):1676–1690. [PubMed: 20172780]
6. Al-Kofahi Y, Lassoued W, Lee W, Roysam B. Improved automatic detection and segmentation of cell nuclei in histopathology images. *IEEE Transactions on Biomedical Engineering*. 2010; 57(4): 841–852. [PubMed: 19884070]
7. Xing, Fuyong; Yang, Lin. Robust selection-based sparse shape model for lung cancer image segmentation. *Medical Image Computing and Computer-Assisted Intervention MICCAI 2013*. 2013; 8151
8. LeCun Y, Bottou L, Bengio Y, Haffner P. Gradient-based learning applied to document recognition. *Proceedings of the IEEE*. 1998; 86(11):2278–2324.
9. Krizhevsky, Alex; Sutskever, Ilya; Hinton, Geoffrey E. Imagenet classification with deep convolutional neural networks. In: Pereira, F.; Burges, CJC.; Bottou, L.; Weinberger, KQ., editors. *Advances in Neural Information Processing Systems 25*. Curran Associates, Inc.; 2012. p. 1097-1105.
10. Zhou, Yin; Chang, Hang; Barner, K.; Spellman, P.; Parvin, B. Classification of histology sections via multispectral convolutional sparse coding. *Computer Vision and Pattern Recognition (CVPR), 2014 IEEE Conference on*. Jun.2014 :3081–3088.
11. Karpathy, Andrej; Toderici, George; Shetty, Sanketh; Leung, Thomas; Sukthankar, Rahul; Fei-Fei, Li. Large-scale video classification with convolutional neural networks. *Proceedings of International Computer Vision and Pattern Recognition (CVPR 2014)*. 2014
12. Chang, Hang; Zhou, Yin; Borowsky, Alexander; Barner, Kenneth; Spellman, Paul; Parvin, Bahram. Stacked predictive sparse decomposition for classification of histology sections. *International Journal of Computer Vision*. 2014:1–16.
13. Chang, Hang; Borowsky, Alexander; Spellman, Paul; Parvin, Bahram. Classification of tumor histology via morphometric context. *Proceedings of the Conference on Computer Vision and Pattern Recognition*. 2013:2203–2210.
14. Huang, Heng; Ding, C.; Kong, Deguang; Zhao, Haifeng. Multi-label relief and f-statistic feature selections for image annotation. *2013 IEEE Conference on Computer Vision and Pattern Recognition*. 2012; 0:2352–2359.
15. Le, Quoc V.; Ngiam, Jiquan; Coates, Adam; Lahiri, Abhik; Prochnow, Bobby; Ng, Andrew Y. On optimization methods for deep learning. *Proceedings of the 28th International Conference on Machine Learning (ICML)*. 2011:265–272.
16. Shewchuk, Jonathan R. Tech Rep. Pittsburgh, PA, USA: 1994. An introduction to the conjugate gradient method without the agonizing pain.
17. Zeiler MD, Taylor GW, Fergus R. Adaptive deconvolutional networks for mid and high level feature learning. *Computer Vision (ICCV), 2011 IEEE International Conference on*. 2011:2018–2025.
18. Bristow, Hilton; Eriksson, Anders; Lucey, Simon. Fast convolutional sparse coding. *Computer Vision and Pattern Recognition (CVPR), 2013 IEEE Conference on*. 2013:391–398.

19. Ruifork A, Johnston D. Quantification of histochemical staining by color decomposition. *Anal Quant Cytol Histology*. 2001; 23(4):291–299.
20. Chang, Hang; Fontenay, Gerald; Han, Ju; Cong, Ge; Baehner, Fredrick; Gray, Joe; Spellman, Paul; Parvin, Bahram. Morphometric analysis of TCGA Glioblastoma Multiforme. *BMC Bioinformatics*. 2011; 12(1)
21. Chang, Hang; Han, Ju; Borowsky, Alexander; Loss, Leandro; Gray, Jow W.; Spellman, Paul T.; Parvin, Bahram. Invariant delineation of nuclear architecture in glioblastoma multiforme for clinical and molecular association. *IEEE Transactions on Medical Imaging*. 2013; 32(4):670–682. [PubMed: 23221815]
22. Kothari S, Phan JH, Osunkoya AO, Wang MD. Biological interpretation of morphological patterns in histopathological whole slide images. *ACM Conference on Bioinformatics, Computational Biology and Biomedicine*. 2012

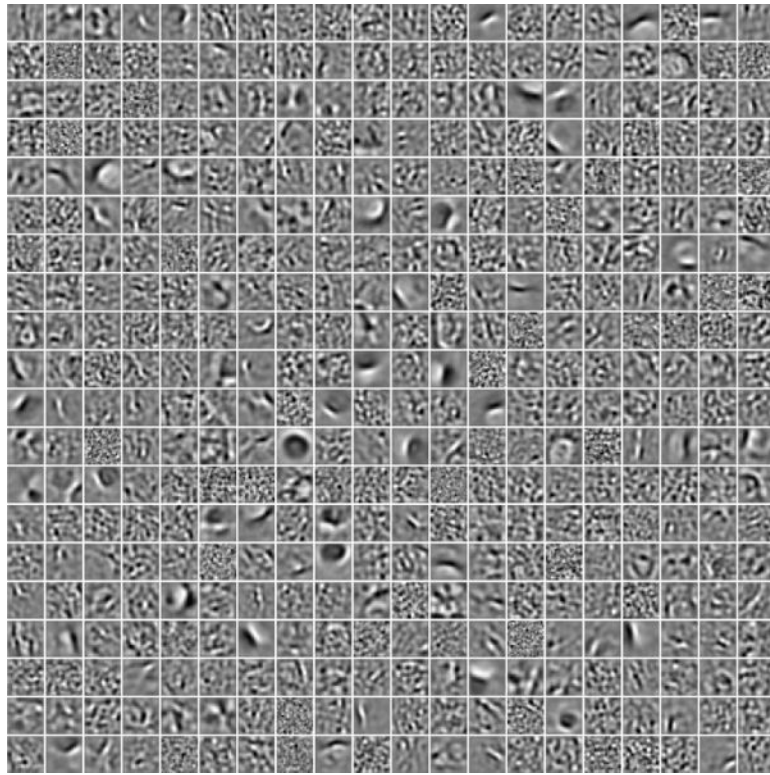


Fig. 1.
21 \times 21 filters learned from the TCGA segmentation benchmark dataset.

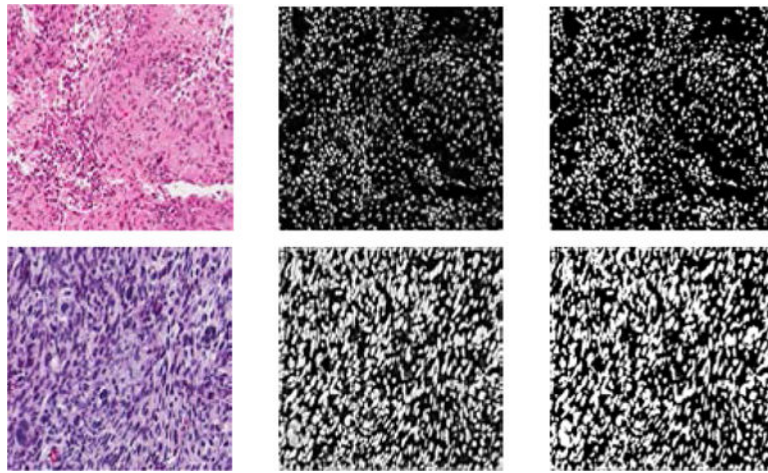


Fig. 2. GBM Examples. First column: original images. Second column: predictions by SCCR. Third column: final segmentation results.

Table 1

Comparison of Segmentation Results.

Method	Precision	Recall	F-Score
SCCR	0.77	0.81	0.790
MRGC-MultiScale [21]	0.77	0.82	0.794
MRGC [21]	0.79	0.78	0.785
Chang <i>et al.</i> [20]	0.78	0.65	0.709
Sonal <i>et al.</i> [22]	0.69	0.75	0.719

Author Manuscript

Author Manuscript

Author Manuscript

Author Manuscript